

Micro Tool Fabrications Through Electrochemical Spark Machining Process

Niladri Mandal[§], Nitesh Kumar^{#,*} and Alok Kumar Das[#]

[§]Defence Research and Development Laboratory (DRDL), Hyderabad-500058, India

[#]Department of Mechanical Engineering, IIT (ISM), Dhanbad, 826004, India,

*E-mail: niladri.drdl@gov.in

ABSTRACT

This article investigates the feasibility of producing an in-situ micro tool rod using micro-electrochemical spark machining (μ -ECSM) technology. The study included the examination of both electrical factors (such as voltage and duty factor) and non-electrical factors (such as electrolyte concentration and spindle speed) as the input parameters for the machining process. The responses measured in the study were the reduction in tool diameter and the surface roughness of the micro tool produced. The potassium hydroxide solution is used as a working fluid. The results indicate that voltage is the most crucial factor that influences micro tool fabrication. The utmost reduction in tool diameter, measuring 279.5 μm , occurred when utilizing machining parameters of 35V, 30%, 4 wt.%, and 600 rpm. Meanwhile, the lowest surface roughness for the micro tool was 3.42 μm , achieved with machining parameters of 35V, 10%, 4 wt.%, and 600 rpm. Additionally, the impact of machining settings on the micro tool electrode is covered.

Keywords: μ -ECSM; Micro tool; Surface roughness; Tungsten

1. INTRODUCTION

The increasing demand for miniature products raises the requirement for micro tool electrodes which can sustain high machining temperatures and have enough strength that it will avoid bending or breaking during the non-contact machining operation¹. Examples of such micro-features might include miniature holes for fiber optics, biomedical filters, micro nozzles utilized in jet engines, and micro molds or dies for either micro optics or microfluidic devices².

Generally, electro-discharge machining (EDM) and electrochemical machining (ECM) processes are widely used for precision machining operations. During the machining, in-situ tool fabrication is most widely used to avoid tool misalignment to other substrates and eliminate run-out errors³. There is various literature on micro tool fabrication using μ -EDM and μ -ECM. Some of the notable works are elaborated on in the succeeding section.

The μ -EDM operation is prominently used to fabricate the micro-electrode⁴. Lim⁵, *et al.* investigated the sacrificial approach to fabricate the high aspect ratio (HAR) of tool rods. De-ionized (DI) water is utilized as a dielectric and tungsten is employed as a tool material with \varnothing 0.5 mm. Since the EDM process is a non-contact machining method, hence it is an easy and feasible way to obtain the HAR tool. They used three different shapes and sizes of sacrificial electrodes. In the first type, they used a stationary block which is simple in the process. In the second approach, a rotating disk is used having a thickness of 0.5 mm and the speed of the rotating disk is approximately 90 rpm. At last, they implemented the wire

electro-discharge grinding (WEDG) method having a wire speed of approx. 3-5 mm/s and wire diameter of 0.07 mm. They revealed that rotating sacrificial disk methods exhibit the best approach to fabricating the HAR tool electrode followed by the stationary sacrificial block and WEDM method. The stationary block methods showed high tool taperness and uneven diameters whereas WEDM depicts high surface roughness of the finished micro tool electrode. Han⁶, *et al.* fabricated a micro tool with tungsten carbide (WC) and super fine powder sintered WC (SWC). They concluded that SWC is capable to fabricate micro-electrodes of diameter 2.8 μm whereas WC attains 4 μm diameter respectively through WEDG methods. Zhang⁷, *et al.* concluded that negative polarity of the machining improves the surface finish of the micro-electrode as compared to positive polarity while machining through tangential feed WEDG (TF-WEDG). However, it shows certain limitations such as thermal stress, micro-cracks, formation of white layer and surface roughness as well as low machining rate (compared to the ECM process) that restrict the researcher to implement this process for the fabrication of the tool⁸.

On the other hand, μ -ECM methods are also used by the researcher to fabricate the micro-electrode tool of HAR in the presence of electrolyte solutions. Patro⁹, *et al.* fabricated a micro tool with an average of \varnothing 60 μm and an aspect ratio of 75 with high carbon steel. They used a 5 % NaCl solution and implemented a FEM-based numerical simulation to evaluate the shape of the tool electrode. Further, they reveal that the most suitable voltage to produce a micro tool was 4V DC showing high reproducibility and precise controllability. In addition, they observed a black (passive) film formed over the tool surface during the machining which helped to make the tool

surface smooth and bright. Jain¹⁰, *et al.* reported the fabrication of a micro tool with an average diameter of 80 μm using steel wire with an initial diameter of 1000 μm . They used H_2SO_4 of 0.1M as an electrolyte solution, a pulsed DC voltage of 6V, and a copper rod of diameter 1300 μm as a cathode. They also observed the black-brownish precipitate which they declare $\text{Fe}(\text{OH})_2$ formed during the fabrication process. Similarly, Das¹¹, *et al.* fabricated a cylindrical micro tool of tungsten having $\text{O} 50 \mu\text{m}$ and a length of 800 μm in the presence of a 3M concentration of KOH electrolyte solution. They obtained the smooth surface finish at voltage 18V, pulse on time 1400 ns, and frequency 500 kHz applied for 15 minutes. They use the ECM turning operation for the development of the micro tool electrode. The $\mu\text{-ECM}$ process also depicts other significant factor such as producing burr-free surface without thermal as well as mechanical stress, micro-cracks and redeposits surfaces. However, it is difficult to fabricate the required tool diameter with this process¹²⁻¹³.

In order to short out the above limitation of both the processes i.e. EDM and ECM, and develop the micro-tool, the hybrid machining process is used i.e. micro electrochemical spark machining method. It operates on the principle of both EDM and ECM processes simultaneously¹⁴⁻¹⁵. The suitability of the micro electrochemical spark method to fabricate in-situ micro tool fabrication is still not explored. Hence, the objective of this article is to studies the viability of the $\mu\text{-ECSM}$ method to develop the in-situ micro tool rod for the application of micro-machining operations. Further, examine the effect of different input parameters on the fabrication of the tool by considering the reduced tool diameter and surface roughness of the fabricated tool as responses.

1.1 Principle Of $\mu\text{-ECSM}$ Process

Figure 1 shows the working principle of the $\mu\text{-ECSM}$ process. Two electrodes i.e. anode and cathode are used to perform the machining operation similar to the parent process i.e EDM and ECM process¹⁶⁻¹⁷. The power source employed for the machining operation is the pulse DC power. Mostly, the tool electrode is made a cathode while the auxiliary electrode acts as an anode during the machining of non-conductive material¹⁸. When the potential difference is applied across the tool and auxiliary electrode, the hydrogen gas bubbles are produced which coalesce to form a thin passivation layer across the tool¹⁹. The oxygen bubbles formed at the anode²⁰.

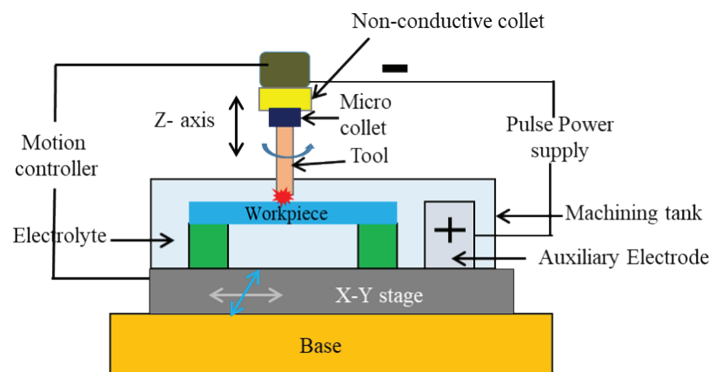


Figure 1. Schematic illustration of the ECSM configuration.

At critical voltage, the passivation film rupture and discharge of sparks occur. Due to this spark energy, the work-piece kept near the tool tip melted and vaporized²¹⁻²².

2. EXPERIMENTATION

A tungsten rod of $\text{O} 500 \mu\text{m}$ is used as a tool. The physical properties of the tool i.e. melting point 3370 $^{\circ}\text{C}$, electrical resistivity 5.65×10^{-6} ohm-cm, specific heat capacitance 0.134 J/g $^{\circ}\text{C}$, and thermal conductivity 163.3 W/mK²³⁻²⁴. The Energy-dispersive X-ray spectroscopy (EDS) confirms the chemical composition of the tool. A rectangular block of high-speed steel (HSS) having the dimension of 50 mm x 10 mm x 30 mm is used as a cathode. A micro tool rod is made using a custom-built $\mu\text{-ECSM}$ system (as shown in Fig. 2).

Initially, the tool (tungsten) rod surface is cleaned by using an acetone bath through ultra-sonication for 10 min. Then, the tool rod is dried and clamped in the micro collet tightly. The tungsten tool rod is made anode. High-speed steel is made cathode (i.e. auxiliary electrode). Its surfaces are cleaned by grinding operation to maintain per-pendicularity and flatness within 0.005 mm. Next, the same has been clamped inside the chamber and dialled to maintain is parallel to the tool (tungsten) rod and connected to the negative terminal. The side flat surface of the auxiliary electrode is maintained an approximately 30 μm inter-electrode gap with the tool rod. For maintaining this micro gap, initially, the tool rod is made to touch the cathode's flat surface before retracting 30 μm away from the cathode's surface with the help of a controller^{12, 25}.



Figure 2. In-house developed $\mu\text{-ECSM}$ setup.

The experiments are performed by considering the approach of one parameter at one time¹⁴. The investigations take into account various machining parameters such as voltage, duty factor, electrolyte concentration, and spindle speed³. The trial experiments are used to select these input parameters and their respective ranges. The potassium hydroxide electrolyte solution is used as a working fluid¹². The other machining parameters are presented in Table 1.

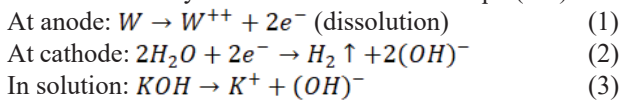
3. FABRICATION OF MICRO-ELECTRODES

An illustration of the method for making micro tools is shown in Fig. 3, in which reverse polarity is applied across the

Table 1. Machining parameters for tool fabrication

Machining parameters	Levels
Voltage (V)	25-45V
Duty factor (DF)	10 - 30 %
Electrolyte concentration (EC)	4 to 12 wt%
Spindle speed (S)	200 to 1000 rpm
Pulse frequency	10 kHz
Electrolyte	KOH
Inter electrode gap	30 μm
Cross feed	40 mm/min

machining cell. A passive film forming across the tool electrode leads to creating potential differences among the anode and cathode and finally resulted in the discharge of sparks. The energy produced by the spark causes the melting and vaporization of the tool. Simultaneously, the electrochemical reaction leads to the chemical etching of the anode surface which shrinks the irregularities and surface roughness formed by the spark erosion²⁶. The possible electrochemical reactions involved during tool fabrication operation between tool electrode and electrolyte solution are shown in Eqn. (1-3)



To investigate the capability of the μ-ECSM process for micro tool fabrication, the reduction in tool diameter and surface roughness of the fabricated tool is analyzed. Based on experimental Table 2, all the experiments were carried out. To monitor the machining process, the digital microscope (Make: Dinolite) is integrated with the setup which helps to visualize the process of machining. The machining duration (180 sec), and inter-electrode gap (30μm) are maintained uniformly for all the experiments.

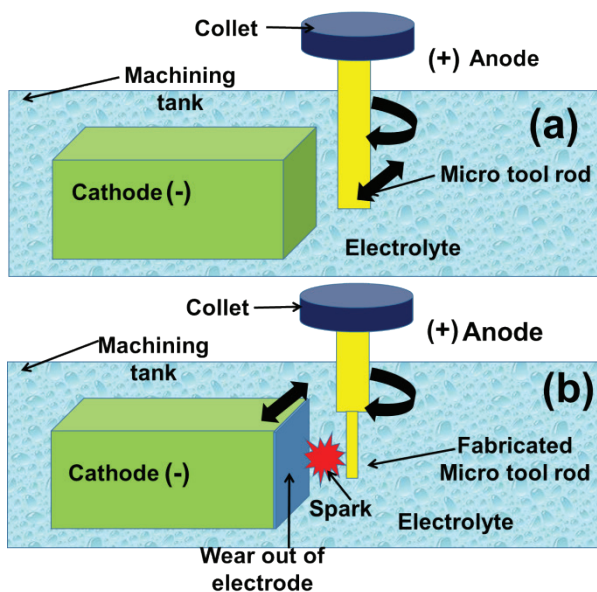


Figure 3. Schematic diagram for fabrication of micro rod through μ-ECSM process (a) at the beginning of the process and (b) fabricated micro tool rod.

4. RESULTS AND DISCUSSION

The fabricated tool is initially cleaned with distilled water to get rid of the debris particles sticking to the tool’s surface. The tool was dried in an oven at 60 °C for 30 min to eliminate the moisture from the surface. Then the diameter of the tool is measured by using a FESEM image through Image J software. The average of measured five diameter readings is recorded and considered as the final reduced diameter.

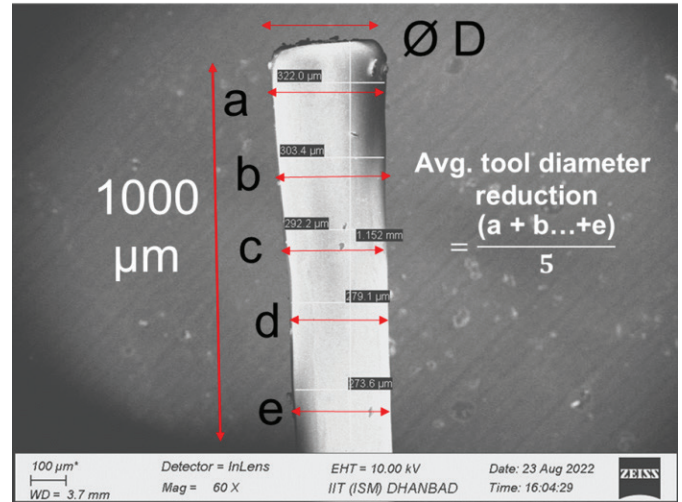


Figure 4. Illustration for measuring the diameter of a fabricated microtool.

All the diameters are measured up to 1000 μm (from the tip of the tool) of the tool length to maintain uniformity in the reading. The details of the diameter measuring methodology are depicted in Fig. 4.

4.1 Tool Diameter Reduction Rate

The average diameter of the fabricated tool is recorded and presented in Table 2. Using this data, the reduction in average tool diameter for the different input parameters is analyzed (Fig. 5 (a-d)). It has been noted that by raising the voltage from 25V to 40V, the average tool diameter is significantly reduced from 384 μm to 337 μm. The shape of the fabricated tool is almost cylindrical with a minute deviation along the axial length (up to 1000 μm).

However on further increment in the voltage (at 45V) tends to the formation of a conical shape of the tool electrode (as observed from the FESEM image Fig. 6). This can be explained by the fact that when the voltage rises, bubble formation rate accelerates which enhances the spark intensity²⁷ and material being removed mainly by sparking and erosion up to 45V. On further increase in the voltage 45V, the chemical action is more dominating as compared to the spark erosion, resulting in conical shape tool formation^{14,17}. Since, the diameter of the conical shape electrode has a large deviation, hence calculating the accurate average reduced diameter of the fabricated tool is quite difficult. Hence, in figure 6, the reduced diameter of the fabricated tool at 45 V is not considered.

In Fig. 7, the average diameter of the reduced tool fabricated at different duty factors ranges from 10 % to 30 %. However, above the 20 % duty factor, a drastic reduction in the average tool diameter is observed.

Table 2. Experimental layout and respective response

Applied voltage (V)	Duty factor (%)	Electrolyte concentration (wt.%)	Spindle speed (rpm)	Tool diameter (μm)	Surface roughness (μm)
25	20	4	600	384.44	3.616
30				374.96	5.139
35				371.06	7.09
40				337.56	7.23
45				155.98	8.595
35	10	4	600	386.68	3.416
	15			382.6	5.218
	20			371.06	5.943
	25			294.06	6.331
	30			279.5	7.71
35	20	4	600	371.06	4.059
		6		249.02	4.616
		8		189.48	6.568
		10		189.72	9.4
		12		120.5	10.994
35	20	4	200	344.26	5.995
			400	371.06	5.468
			600	377.82	3.616
			800	392	5.939
			1000	407.96	6.429

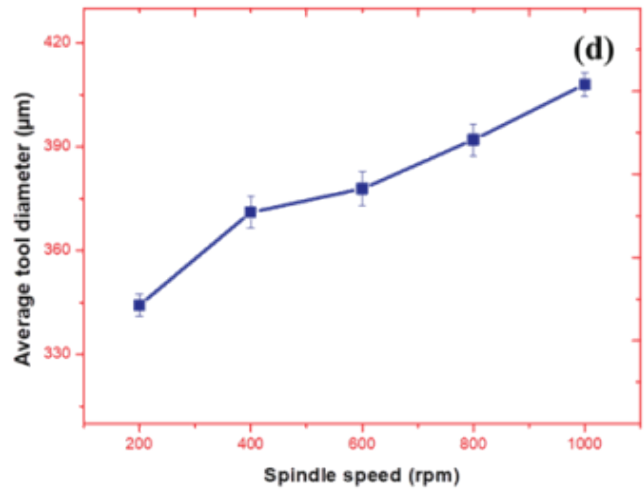
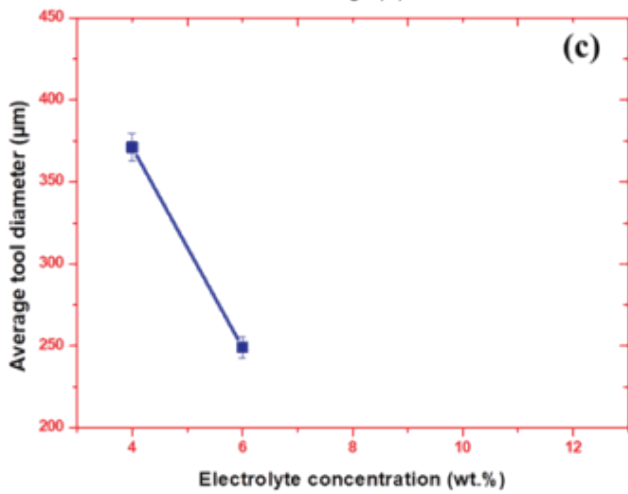
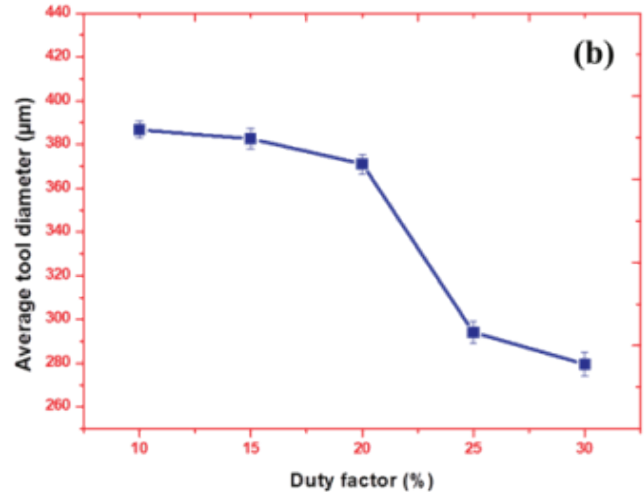
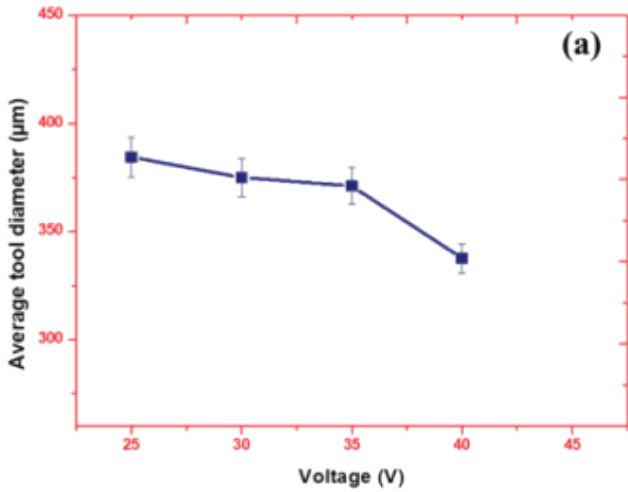


Figure 5. Average reduced tool diameter after fabrication with respect to different input machining parameters.

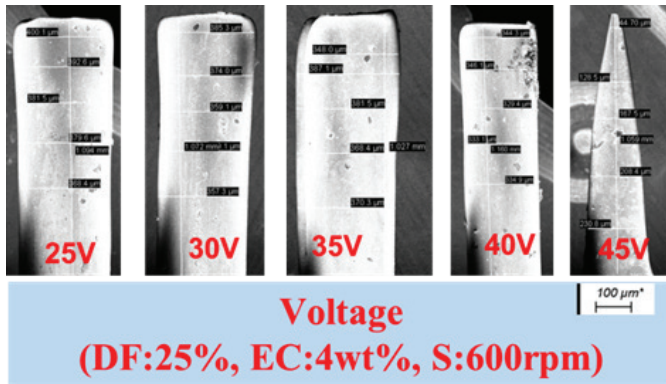


Figure 6. FESEM image of the fabricated micro tool at applied voltage 25V to 45V.

This can be explained as increasing the duration of the power supply, increases the rate of chemical reaction, which causes intense sparks across the tool electrode followed by chemical dissolution of the tool electrode²⁸. The FESEM image (Fig. 7) of the fabricated tool depict all the produced tool are nearly cylindrical in shape. The minimum average diameter of the fabricated tool is 279.5 μm at 30% duty factor, 35V applied voltage, 4 wt.% electrolyte concentration, and 600 rpm spindle speed.

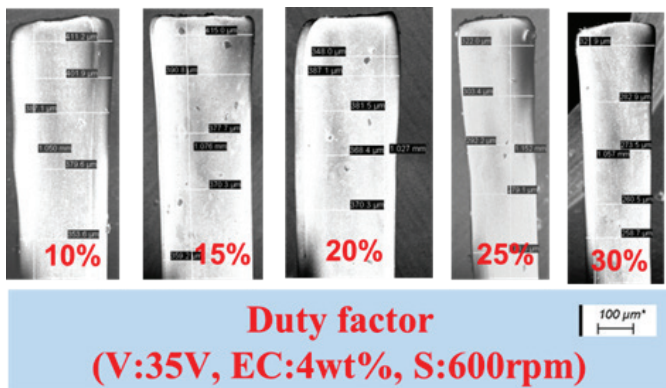


Figure 7. FESEM image of the fabricated micro tool at applied DF: 10 % to 30 %.

In the case of varying the electrolyte concentration from 4 wt.% to 6 wt.% significant neck formation occurs at the electrolyte and air interference. On further increasing the concentration i.e. from 6 wt.% to 12 wt.%, the conical shape of the tool is fabricated (as observed in FESEM image Fig. 8). Chemical reaction contributes to the reduction of tool diameter due to enhancement in chemical etching of the tool¹⁴. The etch rate increases with an increase in presence of OH⁻ ions, which increases with rises in the concentration of KOH in the solutions. The sharp reduction in tool diameter is observed in 8 wt.% and onward concentrations. Hence, electrochemical dissolution action becomes prominent along with the discharge action and results in a conical shape electrode. In addition, the OH⁻ ions enhance with concentration rise which causes a higher etch rate²⁹. As stated in the above section that there is a wide deviation in the average tool diameter measurement and also an unavailability of the appropriate approach. Hence, the average diameter of the fabricated micro tool by varying the electrolyte concentration from 8 wt.% to 12 wt.% are not considered for the average tool diameter analysis.

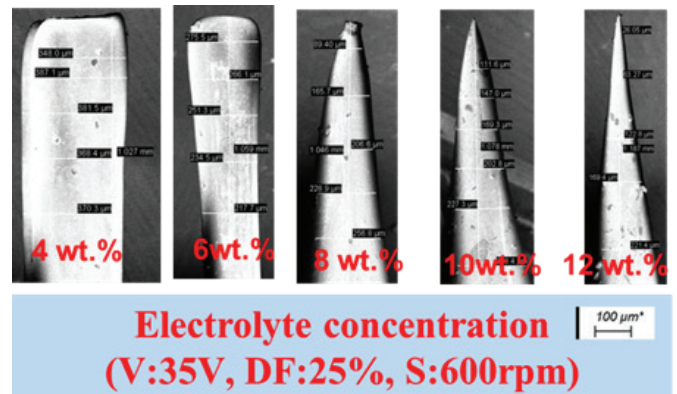


Figure 8. FESEM image of the fabricated micro tool at applied EC: 4wt % to 12wt %.

On the other hand, increasing the spindle speed from 200 rpm to 1200 rpm, the tool diameter reduction rate deteriorated with the rise in spindle speed at constant machining parameters i.e. machining voltage: 35V; DF:20%; and EC: 4 wt.% (Fig. 9). Since increasing the spindle speed, rises the centrifugal force on the bubbles produced near the tool surface. This tends to the formation of an unsteady gas film on the tool surface and deteriorated the intensity of the sparks discharge. Simultaneously, the partial absence of electrolytes over the tool reduces the electrochemical dissolution process¹⁶. Hence, less reduction in tool diameter is observed.

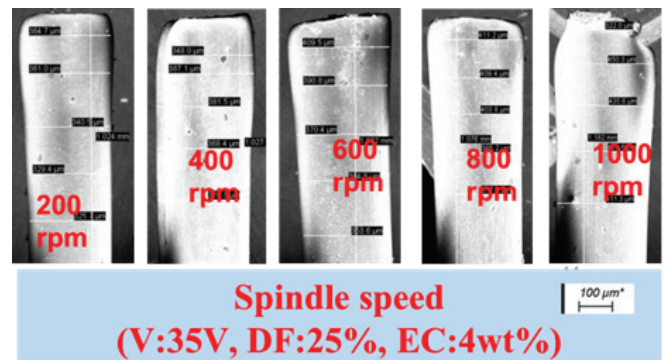


Figure 9. FESEM image of the fabricated micro tool at applied spindle speed: 200 rpm to 1000 rpm.

4.2 Surface Roughness of Tool Diameter for Machining Parameters

The surface roughness of the fabricated tool is measured through a non-contact profilometer. The axial length of 1000 μm from the tip of the developed tool is considered for measuring surface roughness. The micro tool fabrication has been performed by simultaneous action of micro-electro discharge and electrochemical dissolution. Due to micro discharge, surface defects occur over the tool surface such as the formation of the micro crater, voids, melted globules, etc. It has been noticed that a raise in voltage (Fig. 10 a), the surface roughness shows an increasing trend and it varies from 3.6 μm to 8.6 μm at constant machining parameters DF: 20%, EC: 4 wt. %, S: 600 rpm. With increasing the voltage, the heat supplied (P) by discharge increases (Eqn 4³⁰⁻³¹) which directly influenced the surface quality of the fabricated tool.

$$P = (V - V_d)I - RI^2 \quad (4)$$

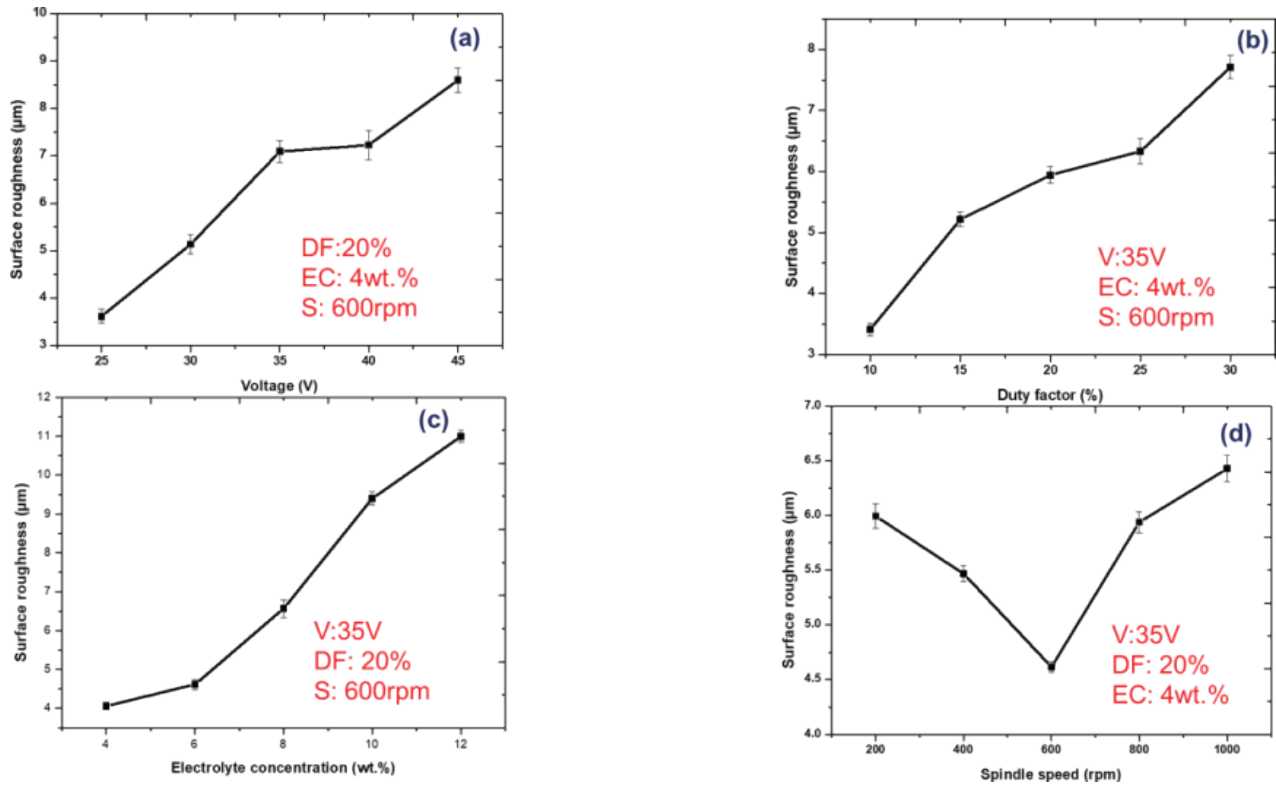


Figure 10. Average surface roughness of fabricated tool surface at different input machining parameters.

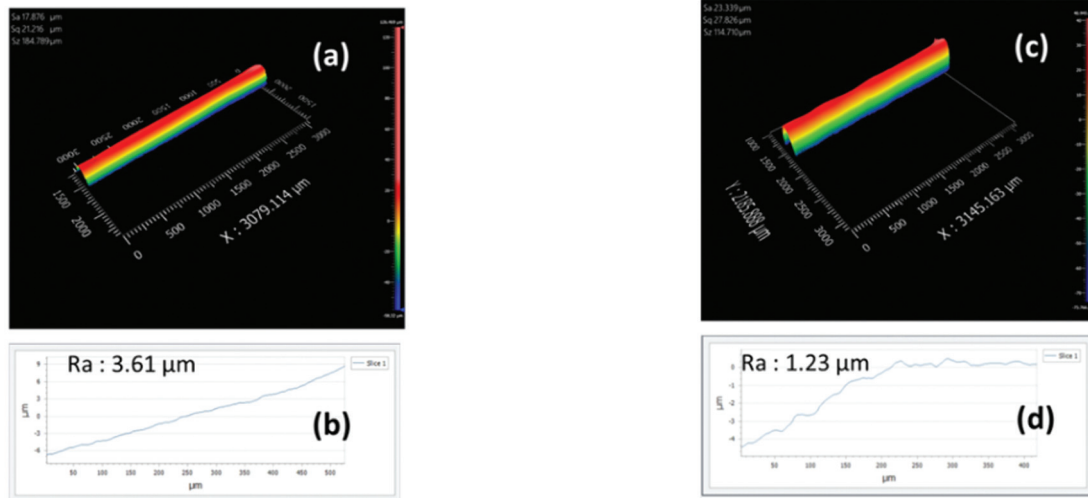


Figure 11. (a, c) 3D surface profile and (b,d) contour curve of fabricated tool.

where, V , I , and R in the above equation depict machining voltage, mean current and inter-electrode resistance. At higher used voltage i.e. 45V, roughness is observed to be 8.6 μm . Since, at this voltage more power is available for machining operation as compared to other used voltages³²⁻³³.

Similar, increasing trends are also observed for the duty factor (DF) as presented in Fig. 10(b). The SR varies from 3.4 μm to 7.7 μm when varying the DF from 10 % to 30 % at constant machining parameters V : 35V, EC : 4 wt.%, S : 600 rpm. Increasing the DF, the duration of sparks formation is for longer periods as compared to lower DF³². This causes severe surface defects over the surface of the tool. At lower DF, the availability of the power at the machining zone is less for higher DF, hence minimum SR is observed at lower DF.

With increasing the electrolyte concentration, the inter-electrode resistance decreases. Hence, more power is developed across the tool electrode³³. This tends to develop high-intensity sparks across the tool which create the surface defect over the tool surface and rises the surface roughness²⁹. Figure 10 (c) depicts the measured surface roughness (SR) of the fabricated tool for different electrolyte concentrations varying from 4 wt. % to 12 wt. % (at constant machining parameters voltage: 35 V, DF: 20%, and spindle speed: 600 rpm). The SR varies from 4.1 μm (at 4 wt. %) to 10.9 μm (at 12 wt. %) in the used machining ranges.

In the case of increasing the spindle speed, the SR initially decreases up to a certain speed and after that, it starts increasing (Fig.10(d)). Similar observations were reported by

another researcher also³⁴⁻³⁵. In used machining parameters, the SR decreases to 3.6 μm at 600 rpm and then increases to 6.4 μm at constant machining parameters i.e. voltage: 35 V, DF: 20 %, and concentration: 4 wt%. This can be elaborated as increasing the spindle speed to 600 rpm, the discharge of spark is concentrated mainly at the tip of the tool electrode and minimizing the occurrence of side sparks. This helps to reduce the surface defects (caused mainly due to spark erosion) over the fabricated tool. On further (above 600 rpm) increment in tool rotation speed the SR increases significantly. This may be due to an increase in centrifugal force which restricts the adhering of the gas bubbles uniformly on the tool surface. This leads to the formation of unsteady discharge across the tool electrode and results in a defective surface³⁶.

The 3D surface profile and contour curve is also captured and few of them are presented in Fig. 11, obtained at machining parameters (a,b) 25V, DF: 20 %, EC: 4wt% and S :600rpm; (c,d) 35V, DF: 10 %, EC: 4wt% and S :600rpm.

5. CONCLUSIONS

- When the machining voltage exceeded 40V, the fabricated micro tools exhibited a conical shape, with all other parameters held constant, including duty factor (20%), electrolyte concentration (4 wt%), and spindle speed (600rpm)
- In the present selected ranges of parameters, the duty factor and spindle speed variation do not lead to the formation of conical-shaped tools while maintaining the other parameters at constant levels i.e. V:35V, EC:4wt%, S:600 rpm, and V:35V, EC:4 wt%, DF:20 %
- The surface roughness of the fabricated tool ranged from 3.4 μm to 11 μm . However, the lowest surface roughness was observed at parameter settings of V:35V, EC:4wt%, DF:10%, and S:600rpm
- As the electrolyte concentration increases, it promotes greater electrochemical dissolution of the tool electrode, accompanied by the discharge of intense sparks around the tool. This process results in the formation of microelectrodes with a conical shape and a rough surface
- Increasing the spindle speed beyond 600 rpm increases the surface roughness due to inconsistent gas film formation.

REFERENCES

1. Kumar, N. & Das, A. K. Critical review on tool wear and its significance on the μ -ECSM process. *Proc IMechE, Part C: J. Mech. Eng. Sci.*, 2023. doi:10.1177/09544062231179988
2. Kumar, N. & Das, A.K. Investigation of tool wear rate during micro-electrochemical spark machining process. *Proc IMechE, Part E: J. Process Mech. Eng.*, 2023. doi:10.1177/09544062231179988
3. Kumar, N.; Mandal, N. & Das, A.K. Micro-machining through electrochemical discharge processes: A review. *Mater. Manuf. Proc*, 2020,**35**(4),363-404. doi:10.1080/10426914.2020.1711922
4. Kumar, N.; Kumar, B. & Pathak, L.C. Effect of shapes and compositions of spark plasma sintered ZrB₂-C composites on performance as EDM tools. *J. Metall. Mater. Sci.*, 2017, **59**(4), 143-152.
5. Lim, H.S.; Wong, Y.S.; Rahman, M. & Lee, M.E. A study on the machining of high-aspect ratio micro-structures using micro-EDM. *J. Mech. Work. Technol.*, 2003, **140**(1-3), 318-325. doi: 10.1016/S0924-0136(03)00760-X
6. Han, F.; Yamada, Y.; Kawakami, T. & Kunieda, M. Experimental attempts of sub-micrometer order size machining using micro-EDM. *Precis. Eng.*, 2006, **30**(2), 123-131. doi: 10.1016/j.precisioneng.2005.06.005
7. Zhang, L.; Tong, H. & Li, Y. Precision machining of micro tool electrodes in micro EDM for drilling array micro holes. *Precis. Eng.*, 2015, **39**, 100-106. doi: 10.1016/j.precisioneng.2014.07.010
8. Sheu, D. Y. High-speed micro electrode tool fabrication by a twin-wire EDM system. *J. Micromech. Microeng.*, 2008, **18**(10), 105014. doi: 10.1088/0960-1317/18/10/105014
9. Patro, S.K.; Mishra, D. K.; Arab, J. & Dixit, P. Numerical and experimental analysis of high-aspect-ratio micro-tool electrode fabrication using controlled electrochemical machining. *J. Appl. Electrochem.*, 2020, **50**(2), 169-184. doi: 10.1007/s10800-019-01380-5
10. Jain, V.K.; Kalia, S.; Sidpara, A. & Kulkarni, V.N. Fabrication of micro-features and micro-tools using electrochemical micromachining. *Int. J. Adv. Manuf. Technol.*, 2012, **61**(9), 1175-1183.
11. Das, A.K. & Saha, P. Fabrication of cylindrical micro tools by micro electrochemical form turning operation. *Proc. Inst. Mech. Eng., Part B*, 2014, **228** (1), 74-81. doi: 10.1177/0954405413497007
12. Das, A.K. & Saha, P. Analysis on fabrication of micro-tools by micro-electrochemical machining process. *Int. J. Nanomanuf.*, 2013, **9**(1), 66-76.
13. Rahman, M.Z.; Das, A.K. & Chattopadhyaya, S. Fabrication of high aspect-ratio tungsten microtools through controlled electrochemical etching. *Mater. Manuf. Processes*, 2021, **36**(11), 1236-1247. doi:10.1080/10426914.2021.1905834
14. Kumar, N. & Das, A.K. Machining of micro features through μ -ECSM process and evaluation of surface integrity. *CIRP. J. Manuf. Sci. Technol.*, 2022, **36**, 45-56. doi: 10.1016/j.cirpj.2021.11.001
15. Kumar, N.; Bishwakarma, H.; Sharma, P.; Singh, P.K. & Das, A.K. Optimization of process parameters in micro-electrochemical discharge machining by using grey relational analysis. *Mat. Sci. Forum*, 2020, **978**, 121-132. Trans Tech Publications Ltd.
16. Islam, M.J.; Zhang, Y.; Zhao, L.; Yang, W. & Bian, H. Material wear of the tool electrode and metal workpiece in electrochemical discharge machining. *Wear*, 2022, **500**, 204346. doi: 10.1016/j.wear.2022.204346
17. Kumar, N.; Mandal, N. & Das, A.K. Microelectrochemical sparks machining: a modern approach for fabrication of microcomponents from nonconductive materials. In *Micro electro-fabrication*, 2021, pp. 277-315.

18. Kumar, N. & Das, A.K. Micro-channel fabrication on GFRP composite through electrochemical spark machining method and optimization of process parameters. *Proc. Inst. Mech. Eng., Part B*, 2022, 09544054221093302. doi: 10.1177/09544054221093302
19. Singh, T. & Divedi, A. Fabrication of micro holes in Ytria-stabilized zirconia (Y-SZ) by hybrid process of electrochemical discharge machining (ECDM). *Cera. Int.*, 2021, **47**(16), 23677-23681. doi: 10.1016/j.ceramint.2021.05.017
20. Harugade, M.; Waigaonkar, S. & Dhawale, N. A novel approach for removal of delaminated fibers of a reinforced composites using electrochemical discharge machining. *Proc. Inst. Mech. Eng., Part B*, 2021, **235**(12), 1949-1960. doi: 10.1177/09544054211014483
21. Sarkar, B.R.; Doloi, B. & Bhattacharyya, B. Parametric analysis on electrochemical discharge machining of silicon nitride ceramics. *Int. J. Adv. Manuf. Tech.*, 2006, **28**(9), 873-881. doi: 10.1007/s00170-004-2448-1
22. Zhao, D.; Zhu, H.; Zhang, Z.; Xu, K.; Gao, J.; Dai, X. & Huang, L. Influence of electrochemical discharge machining parameters on machining quality of microstructure. *Int. J. Adv. Manuf. Technol.*, 2022, 1-14. doi: 10.1007/s00170-021-08316-4
23. Teimouri, R. & Baseri, H. Study of tool wear and overcut in EDM process with rotary tool and magnetic field. *Adv. Tribol.*, 2012.
24. Jain, A.; Singh, B. & Shrivastava, Y. Reducing the heat-affected zone during the laser beam drilling of basalt-glass hybrid composite. *Comp. Part B*, 2019, **176**, 107294. doi: 10.1016/j.compositesb.2019.107294
25. Mandal, N.; Kumar, N. & Das, A.K. Machining of Maraging Steel Through Al₂O₃ Abrasive Powder Assisted Electrochemical Discharge Machining. In *Advances in Modern Machining Processes: Proceedings of AIMTDR 2021*, pp. 101-110. Singapore: Springer Nature Singapore. 2022.
26. Kumar, N.; Bishwakarma, H.; Anand, M.; Tyagi, R. & Das, A. K. Fabrication of micro-channels using a micro-electrochemical spark machining process. *Mat. Today Proc.*, 2022. doi:10.1016/j.matpr.2022.11.188
27. Krötz, H. & Wegener, K. Sparc assisted electrochemical machining: a novel possibility for microdrilling into electrical conductive materials using the electrochemical discharge phenomenon. *Int. J. Adv. Manuf. Technol.*, 2015 **79**(9-12), 1633-1643.
28. Sabahi, N. & Razfar, M.R. Investigating the effect of mixed alkaline electrolyte (NaOH+ KOH) on the improvement of machining efficiency in 2D electrochemical discharge machining (ECDM). *Int. J. Adv. Manuf. Technol.*, 2018, **95**, 643-657. doi: 10.1007/s00170-017-1210-4
29. Jui, S.K.; Kamaraj, A.B. & Sundaram, M.M. High aspect ratio micromachining of glass by electrochemical discharge machining (ECDM). *J. Manuf. Proc.*, 2013, **15**(4), 460-466. doi: 10.1016/j.jmapro.2013.05.006
30. Fascio, V.; Wüthrich, R. & Bleuler, H. Spark assisted chemical engraving in the light of electrochemistry. *Electrochimica Acta*, 2004, **49**(22-23), 3997-4003. doi: 10.1016/j.electacta.2003.12.062
31. Jain, V.K.; Dixit, P.M. & Pandey, P.M. On the analysis of the electrochemical spark machining process. *Int. J. Mach. Tools Manuf.*, 1999, **39**(1), 165-186. doi: 10.1016/S0890-6955(98)00010-8
32. Kim, D.J.; Ahn, Y.; Lee, S.H. & Kim, Y.K. Voltage pulse frequency and duty ratio effects in an electrochemical discharge microdrilling process of Pyrex glass. *Int. J. Mach. Tools Manuf.*, 2006, **46**(10), 1064-1067. doi:10.1016/j.ijmachtools.2005.08.011
33. Behroozfar, A. & Razfar, M.R. Experimental study of the tool wear during the electrochemical discharge machining. *Mater. Manuf. Processes*, 2016, **31**(5), 574-580.
34. Zheng, Z.P.; Su, H.C.; Huang, F.Y. & Yan, B.H. The tool geometrical shape and pulse-off time of pulse voltage effects in a Pyrex glass electrochemical discharge microdrilling process. *J. Micromech. Microeng.*, 2007, **17**(2), 265. doi: 10.1088/0960-1317/17/2/012
35. Gautam, N. & Jain, V.K. Experimental investigations into ECSD process using various tool kinematics. *Int. J. Mach. Tools Manuf.*, 1998, **38**(1-2), 15-27. doi: 10.1016/S0890-6955(98)00034-0
36. Yang, C.K.; Wu, K.L.; Hung, J.C.; Lee, S.M.; Lin, J.C. & Yan, B.H. Enhancement of ECDM efficiency and accuracy by spherical tool electrode. *Int. J. Mach. Tools Manuf.*, 2011, **51**(6), 528-535. doi: 10.1016/j.ijmachtools.2011.03.001

CONTRIBUTORS

Dr Niladri Mandal is Scientist F and working at DRDO-DRDL, Hyderabad. His current contribution is involved in planning and conducting all the experiments.

Dr Nitesh Kumar obtained his Ph.D. in hybrid micro manufacturing from IIT(ISM) Dhanbad. He is working as Senior Research Fellow at IIT(ISM) Dhanbad. His contribution in present study involves the analysis and initial drafting of the manuscript.

Prof. Alok Kumar Das is an Associate Professor at IIT(ISM) Dhanbad. His area of research is micro machining, laser assisted micro machining, surface modification, hybrid manufacturing, additive manufacturing. His contribution in the present study is to supervise the investigation and final editing of the manuscript.